Combustion and Flame 260 (2024) 113095

Contents lists available at ScienceDirect

Combustion and Flame

journal homepage: www.sciencedirect.com/journal/combustion-and-flame

Enhanced energy delivery of direct-write fabricated reactive materials with energetic graphene oxide

Haiyang Wang [a], Yue Jiang [b], Yujie Wang [a], Jihyun Baek [b], Xiaolin Zheng [b], Michael R. Zachariah [a,*]

[a] Department of Chemical and Environmental Engineering, University of California, Riverside, CA 92521, USA
[b] Department of Mechanical Engineering, Stanford University, Stanford, CA 94305, USA

ARTICLE INFO

Keywords:
3D printing
Al/CuO
Nanothermite
Heat flux
Graphene oxide

ABSTRACT

Aluminum (Al) based reactive materials are of interest as their addition can significantly increase the energy density of energetic composites such as solid propellants. In this study, we employed graphene oxide (GO) as an energetic gas generator to increase the ignitability of Al and promote the flame propagation of Al/CuO thermite composites. Compared to the pristine Al/CuO composite, 2.5 wt % addition of GO releases gas and heat upon disproportionation, resulting in a 2X higher burn rate and heat flux. Though both GO and reduced graphene oxide (rGO) addition can reduce the agglomeration size of Al NPs by 2X, GO is more energetic with heat and gas release at low temperature, granting it the ability to increase the ignitability of Al NPs and promote the energy delivery of Al/CuO composite. This study provides a simple way to increase the energy delivery rate of reactive materials by adding a small percentage of functionalized carbon nanomaterials.

1. Introduction

Reactive materials are heterogeneous energetic materials that generally contain reactive metal fuels such as aluminum (Al), titanium, and magnesium, and metal oxides based oxygen donors such as CuO, Bi_2O_3, and Fe_2O_3 [1–8]. Reactive materials have attracted great attention as their addition can significantly increase the energy density of energetic composites such as solid propellants and explosives [9,10]. Compared to the conventional micro-sized reactive materials, nanosized reactive materials have much larger diffusion contact areas between the fuel and oxidizer, and hence are expected to release energy at a much higher rate [1,7,11]. However, the enhancement of the energy delivery rate of the reactive materials using nanoparticles for their micro counterparts is not as great as might be expected based on simple geometric considerations [11–15]. The reason behind this is the rapid sintering/agglomeration of Al nanoparticles (NPs) upon heating, which can occur at a rate faster than their combustion time [16–19]. Consequently, Al NPs may actually burn at the microscale or even larger, losing their nano features and high surface area during combustion, and consequently delivering energy at a much lower rate than expected [11,20].

Carbon materials such as graphite flakes, carbon black, carbon fibers, and graphene have been employed to promote the ignitibility and reactivity of reactive materials [21–28]. For example, Shen et al. used graphene as an additive to increase the ignitability and combustion characterizations of Al/CuO nanothermites [27]. Yi et al. used carbon fibers as sensitizers to promote the reaction of Al/Bi_2O_3 [28]. In our recent study, we added carbon fibers into 3D printed Al/CuO nanothermite composites and found them to promote the burn rate by 2X [31]. The reason is that carbon fibers cause agglomerates to be ejected from the burning surface and attach on the fibers, thus providing more heat feedback. However, those carbon fibers themselves are inert and do not contribute to the chemistry of the thermite reaction. This suggests employing carbon nanomaterials with functional energetic groups could be employed for both physical and a chemical promotion. Functionalized energetic graphene materials such as ultrathin graphene oxide (GO) and graphene fluoride (GF) have been found to be effective additives for metal combustion. GO and GF [21,29,30], are considered to provide reactive radicals, heat, and gaseous products at relatively low temperatures, which lower the ignition threshold; reduce particle agglomeration; and promote energy release of Al and boron combustion [21,29,30]. Although efforts have been made using functionalized carbon nanomaterials/functionalized graphene in reactive powder energetic materials, little has been done to investigate the effects of these additives on flame propagation in printed energetic composites.

* Corresponding author.
E-mail addresses: xlzheng@stanford.edu (X. Zheng), mrz@engr.ucr.edu (M.R. Zachariah).

https://doi.org/10.1016/j.combustflame.2023.113095
Received 19 March 2023; Received in revised form 20 September 2023; Accepted 20 September 2023
Available online 21 December 2023

Herein, we employed GO as an energetic gas generator and investigated its effects on the ignitability of Al and the flame propagation properties of Al/CuO thermite composites. We used a direct-ink-write approach to fabricate high loading (90 wt %) Al/CuO nanothermite composites with a 10 % polymer mixture of hydroxypropyl methylcellulose (HPMC) and poly(vinylidene fluoride) (PVDF). With various amounts of GO and rGO addition, the burn rates, flame temperatures, and heat flux of Al/CuO composites are measured. Compared to the pristine Al/CuO composite, GO releases gas and heat upon disproportionation and oxidation, resulting in a doubled burn rate and heat flux with just ~2.5 wt % addition. Unlike the physical effects that the carbon fibers have on the Al/CuO thermite composites [31], the enhancement of GO on the Al combustion performance is mainly owing to its early decomposition, which not only provides heat but also gas to increase the ignitability of Al NPs. We also found the pre-assembling of Al@GO and Al@rGO can reduce the agglomerating/sintering size of aluminum nanoparticles, however, we found that merely physically adding GO also increased the heat flux, indicating that the aggregation status of Al NPs is not important in the flame propagation of Al/CuO composite sticks.

2. Experimental section

2.1. Materials

Aluminum nanoparticles (Al NPs, 72.5 wt. % active, 70 nm) and CuO microparticles (CuO MPs, ~5 μm) were purchased from US Research Nanomaterials and Sigma-Aldrich, respectively. METHOCEL™ F4M Hydroxypropyl Methylcellulose (HPMC) and Polyvinylidene Fluoride (PVDF), average molecular weight: ~534,000) were obtained from Dow Chemical Company and Sigma-Aldrich, respectively. N, N dimethylformamide (DMF, 99.8 %) was purchased from Sigma-Aldrich and used as a solvent to dissolve the above polymers.

2.2. SEM/EDS and TG/DSC

The morphologies and compositions of the carbon fibers and the 3D-printed composite sticks were characterized by scanning electron microscope (SEM, Thermo-Fisher Scientific NNS450) coupled with energy-dispersive X-ray spectroscopy (EDS). Thermogravimetric analysis/differential scanning calorimetry (TGA/DSC, Setaram LABSYS Evo) in this study were conducted in air or argon flow (40 mL/min) at a heating rate of 10 °C/min from room temperature to 1000 °C. For each test, 4 mg of sample powders were placed in a 100 μL alumina crucible. The baseline correction of the sample TGA and DSC curves was performed by subtracting the TGA and DSC curves of the empty alumina crucible with the same heating process.

2.3. Al@GO and Al@rGO preparation

Al@GO (Al content is 90 wt %, and GO is in 10 wt %) composite powders were prepared by a mechanical mixing method. We first dispersed 10 mg of GO powder (0.5–5 μm in diameter, 0.8–1.2 nm in thickness, XFNANO) in ethanol (1 mg/mL) and sonicated for 2 h. Meanwhile, 90 mg of Al nanoparticles (70 nm in diameter, US Nano) were dispersed in 9 mL of ethanol by sonication for 30 min. After that, the GO suspension was added to the Al suspension and sonicated for 1 h. The mixture was filtered and fully dried on a hotplate at 60 °C for 1 h, and subsequently in a vacuum desiccator for 12 h. We used the same method to prepare the mixture of the Al@rGO (90/10 wt %). The rGO was prepared by thermally reducing GO powder in an argon (Ar) environment at 400 °C. rGO is also used as an additive to Al/CuO for a comparison to GO. The scanning electron microscopy (SEM) images of Al NPs, Al@GO, and Al@rGO are shown in Fig. 1a-c, respectively.

2.4. T-Jump ignition and time-of-flight mass spectrum (TOFMS)

Samples of GO, rGO, Al@GO, and Al@rGO for T-Jump ignition and TOFMS were prepared by a physical mixing method. Generally, the sample powder was suspended in hexane for 10 min of sonication. A small amount of the sample was deposited on a thin Pt wire (76 μm diameter, OMEGA Engineering Inc.), which can be resistively heated to 1000 °C for ignition at a rate of ~10^5 K/s. The temporal temperature of

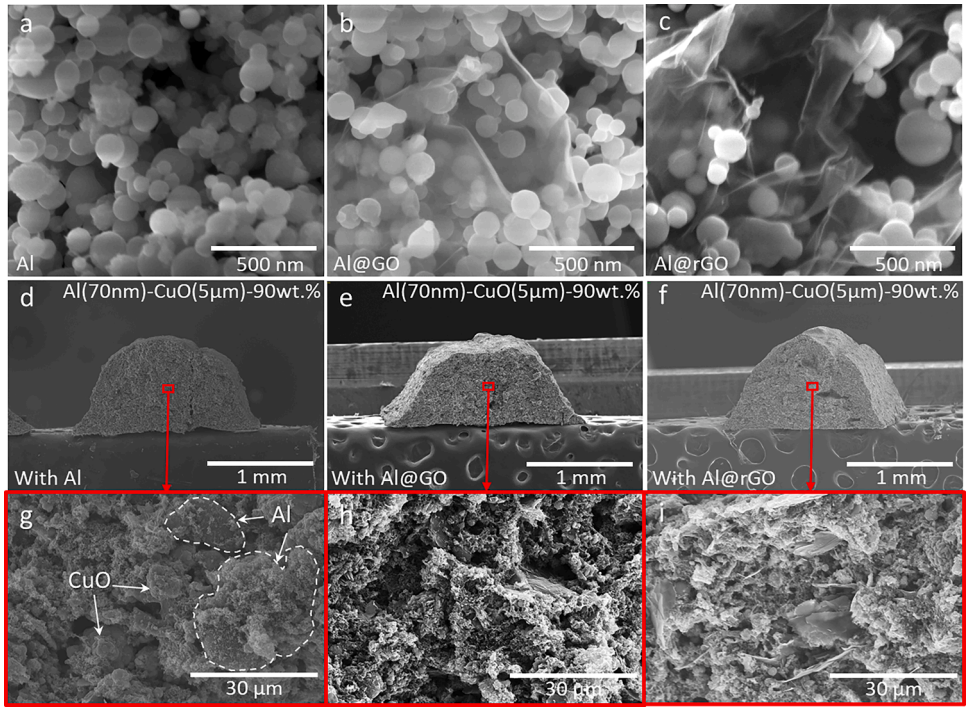

Fig. 1. SEM images of reference Al NPs (a), Al@GO (b), and Al@rGO (c) nanocomposites; lower (d-f) and higher magnification (g-i) SEM images of different Al/CuO composites with the above reference Al (d and g), Al@GO (e and h) and Al@rGO (f and i).

the wire is obtained from the Callendar-Van Dusen equation. The ignition delay time is determined from the video captured with a high-speed camera (Vision Research Phantom V12.1) and the ignition temperature is estimated by correlating the video and the measured wire temperature. The ignition tests are conducted under 1 atm argon or air as noted. The details about T-Jump/TOFMS can be found in our previous studies [32,33].

2.5. Direct-write of Al/CuO nanothermite composite sticks

To prepare the ink for printing, typically 1125 mg Al and CuO, 75 mg HPMC and 50 mg PVDF, and 4 mL DMF were used for each ink formulation. The amount of Al/CuO is reduced when GO or rGO is added in the formulation, but the total polymer loading (10 wt %) remains the same. The details of the formulations are shown in Fig. S1. HPMC and PVDF were dissolved in DMF in a mass ratio of 3:2 to form a clear viscous solution by magnetically stirring the mixture overnight (300 rpm). Then, a measured amount of CuO MPs and Al NPs (with and without GO or rGO, physically added or pre-assembled) was added to the above to form a slurry. A 30 min ultra-sonication step was implemented after each addition of the CuO MPs and Al NPs, respectively, to break up aggregates. The slurries were magnetically stirred (300 rpm) for 24 h to achieve homogenization. The slurries were also mechanically stirred for 1 h prior to printing.

In a typical printing process, the obtained inks were extruded through a 16-gauge needle (inner diameter: 1.35 mm) at a feed rate of ~12 mL/h (extrusion speed of the ink) and a writing speed (moving speed of the nozzle) of 22 cm/min. Printed lines are completely dried before depositing another layer due to the heating of the substrate at 75 °C, and the resulting lines (15 layers) formed a square 8 cm × 8 cm frame with a semicircle cross-section with a diameter of 1 mm. After printing, the samples were left on the heating substrate (75 °C) for additional 30 min to further evaporate any remaining solvent. Finally, the frame was cut into 3 cm long sticks for combustion characterization. The density (mass/volume, ρ) is determined from the mass divided by the volume (cross-sectional area × length) of each stick. The porosity of the samples was estimated by (1-(actual density/theoretical density)). The low and high magnification cross-sectional SEM images of the Al/CuO composites are shown in Fig. 1d-f and g-i, respectively.

2.6. Macroscopic and microscopic imaging systems

As shown in Fig. 2, the printed sticks were placed between two different camera systems that can simultaneously capture the macroscopic and microscopic combustion videos. The macroscopic imaging camera (Vision Research Phantom Miro M110, 13,000 frames/s) has a window size of 256 × 128 pixels, and a resolution of 82 μm/pixel, while the microscopic imaging camera (Vision Research Phantom VEO710L coupled to Infinity Photo-Optical Model K2 DistaMax, 24,000 frames/s) has a window size of 512 × 512 pixels, and a resolution of 2.2 μm/pixel. The sample was fixed by double-sided tape on steel support and was ignited by a thin nichrome wire coil (0.01″ diameter). The burning of the printed sticks was conducted in 1 atm Ar and the burn rate is reported

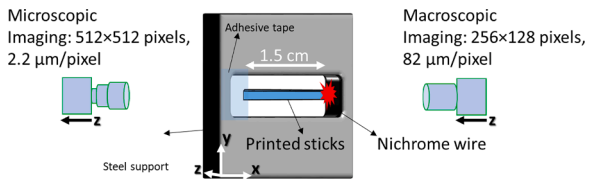

Fig. 2. The macroscopic and microscopic imaging system of observing the flame propagation of an Al/CuO composite stick in an inert environment (1 atm argon). The macroscopic imaging system has a window size of 256 × 128 pixels with a resolution of ~80 μm/pixel while the microscopic imaging system has a window size of 512 × 512 pixels with a resolution of ~2 μm/pixel.

based on three runs of each sample. The linear burn rate rates (ν) and average flame temperature (T) of the composite sticks were determined from the macroscopic videos. The heat flux calculations consider densities (ρ), burn rates (ν) and flame temperatures (Heat flux ~ $\rho \times \nu \times T$) and are normalized based on the Al/CuO composite without the addition of GO or rGO. The details of how we obtained the temperature by color pyrometry can be found in our previous studies [34,35]. Briefly, three-channel intensity (red, green, blue) ratios extracted from the color camera are processed using a house-built MATLAB routine and demosaiced for the camera's Bayer filter using the built-in MATLAB algorithms. The system was calibrated with a blackbody source (Mikron, Oriel) and the corresponding flame temperature maps were output and reported. The temperature uncertainty is estimated to be ~200–300 K.

3. Results and discussion

3.1. Thermochemical property (heat/gas release) of GO and rGO

The thermal decomposition properties of the GO and rGO are shown in Fig. 3. The results in Fig. 3b and d show that GO has an early exothermic peak at 200 °C regardless of the gas environment (Air or Ar) Based on previous studies about thermal reduction of GO [29,36], the GO actually undergoes a so-called disproportionation reaction, in which the partially oxidized sp3 carbon become fully oxidized to carbonaceous gases such as CO_2 and the rest is reduced to sp2 graphene. However, rGO does not have this peak due to the relative lack of oxygen functional groups during the preparation process, as evidenced by the XPS analysis in Figs. S1a and 1b. Correspondingly, as shown in Fig. 3a and c, the mass drop of GO (200–300 °C) is associated with disproportionation, and the slight mass drop of rGO (200–300 °C) may be owing to the slow decomposition of some residual groups. At the higher temperature range, both GO and rGO have a carbon oxidation peak at 400–600 °C in the presence of air (Fig. 3b), where GO's residue is oxidized more rapidly in a one-step process while rGO experiences slower oxidation with two steps. It is also noted that the oxidation of rGO's residue is slightly earlier than that of GO, which can be attributed to the presence of more carbon defects, as suggested by the Raman spectra in Fig. S1c.

The gas release properties of GO, rGO, and their Al NPs containing mixtures are measured in a T-Jump time-of-flight mass spectrum, and the collected spectra are shown in Fig. 4a and b for GO and rGO, respectively. All the spectra are normalized to H_2O ($m/z = 18$). GO releases a much greater amount of CO_2 upon decomposition than rGO, which is not surprising, as GO has ~32 at % O compared to ~16 at % in rGO shown in X-ray photoelectron spectroscopy (XPS) results in Fig. S1. With the increase of GO content in the Al/GO composites, the amount of CO_2 release also increases, further confirming the high gas release from GO. In contrast, rGO and the Al/rGO composites release much less CO_2, and the CO_2 peaks do not increase with the increase of rGO content. We also noticed that the Al2O peaks for Al/GO and Al/rGO composites, are similar to neat Al NPs, implying no direct reaction between Al NPs and GO/rGO.

To explore the effects of GO addition on Al ignition, Al NPs, Al@GO, and Al@rGO composites were coated on a thin platinum wire and heated up to 1000 °C in air. The typical ignition snapshots are shown in Fig. 4c-e. Only Al@GO was successfully ignited while Al NPs just sinter into a big droplet upon heating without ignition. Al@rGO shows some degree of ignition as we observed small sparks flying but it is much less violent. As Fig. 1a-c shows, Al NPs have a high degree of aggregation, while after mixing with GO or rGO, they are dispersed better on the thin carbon sheets and fewer aggregations are observed. More importantly, upon heating, GO releases heat and gas (CO_2) at a relatively low temperature (200 °C), which is much lower than the melting point of Al (660 °C), offering an opportunity to separate the nanoparticles before they can sinter/agglomerate into larger droplets. These well-dispersed nanoparticles when ignited, generate a more violent event.

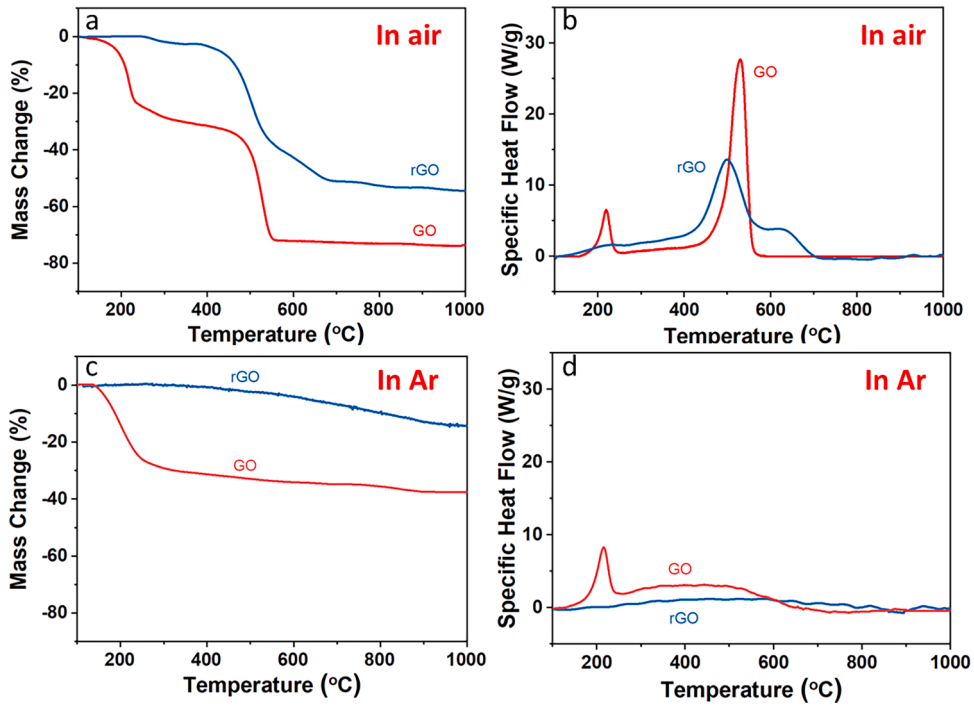

Fig. 3. TGA (a and c) and DSC (b and d) results of GO (a and b) and rGO (c and d) upon heating at a rate of 10 °C/min in the air (a and b) and argon (c and d).

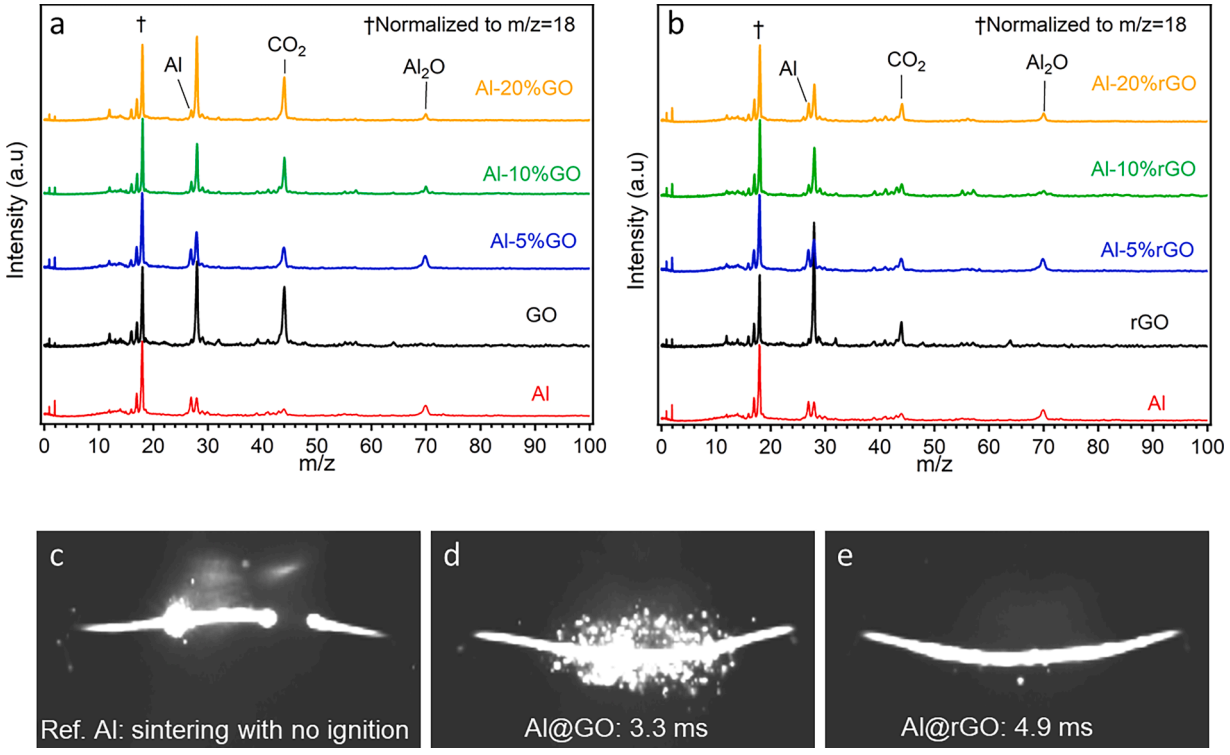

Fig. 4. T-Jump mass spectra of Al NPs, GO, and their mixtures (a) in a vacuum; and the mass spectra of Al NPs, rGO, and their mixtures (b) in a vacuum. T-jump wire ignition of Al NPs (c), Al@GO (d), and Al@rGO (e) in air.

3.2. Effects of Al@GO and Al@rGO addition on the flame propagation of free-standing Al/CuO composites

As GO promotes the ignition of Al NPs, we can incorporate it into the Al/CuO composites to explore its effects on flame propagation. Al@GO and Al@rGO with different GO and rGO contents were mixed with stoichiometric CuO and formulated with a polymer mixture of HPMC/PVDF (10 wt %) to directly write free-standing composite sticks [37]. The cross-sectional SEM images of typical reference Al/CuO, Al@GO/-CuO, and Al@rGO/CuO composite sticks are shown in Fig. 1. The burn rate, flame temperature, and heat flux of different Al/CuO composite sticks with Al@GO and Al@rGO are measured in an argon environment

and the results are shown in Fig. 5a and b, respectively. Fig. 5a shows that the burn rate and heat flux of Al/CuO increase with the increase of GO content from 0 wt % to 2.5 wt %. The Al@GO (2.5 wt %)/CuO has a doubled burn rate and heat flux compared to the reference Al/CuO. When the GO content is further increased to 5 wt %, both the burn rate and heat flux decline, to roughly the same as the reference. By contrast, the burn rate and heat flux of Al/CuO decreases rapidly with the increase of rGO, with a nearly 50 % reduction when the rGO addition is 5 wt % compared to the reference of Al/CuO. For both cases, the measured flame temperatures reduce slightly, with the increase of GO or rGO. GO not only promotes the ignition of Al NPs but also increases the flame propagation rate of Al/CuO composites, which is probably because of the early decomposition of GO that can release heat and gas at the same time.

We also noted that pre-assembly of Al and GO or rGO reduces the aggregations of Al NPs as the SEM images show (Fig. 1). With GO and rGO, Al@GO and Al@rGO are better dispersed with less aggregation compared to bare Al NPs. The role of Al aggregations on the agglomeration formation and flame propagation needs to be further explored.

3.3. *Effects of physical GO, and rGO addition on the flame propagation of free-standing Al/CuO composites*

To better probe the effects of Al aggregation status, GO and rGO were also physically added to the Al/CuO composites for comparison. As we mentioned above, Al@GO and Al@rGO represent the pre-assembled Al NPs/carbon mixtures while Al/GO and Al/rGO refer to simple mixture of the Al NPs and the carbon materials. The above-mentioned pre-assembled Al@GO, Al@rGO, Al/GO, and Al/rGO mixtures were then physically mixed with CuO and the binder, to print the free-standing Al/CuO composite sticks. One thing we noted is that the densities of composite sticks with pre-assembled Al@GO, and Al@rGO are about 13 %−30 % higher than the physically mixed cases (with Al/GO, and Al/rGO) and 13 %−20 % higher than the reference Al/CuO (no GO or rGO cases), respectively, as shown in Fig. 6a, indicating the close assembly between GO or rGO with Al NPs helps to reduce the voids in the printing composites. On the contrast, the porosities of Al/CuO composite sticks with physically mixed Al/GO or Al/rGO is either similar or lower compared to the reference (No GO or rGO), of which, Al/CuO composite with physically mixed Al/rGO is the lowest (61 % porosity), due to the low density of rGO itself (See cross-sectional SEM images in Fig. S2 for more details).

As Fig. 6b shows, GO promotes the burn rate and heat flux by 100 % regardless of if it was pre-assembled or just physically mixed with Al NPs. Apparently, the aggregation state of Al NPs in the composites does not affect the flame propagation of Al/CuO composite sticks with the addition of GO. The addition of rGO also increases the burn rate by almost 100 % but mainly due to its relatively low density (large porosity, Fig. 6a and Fig. S2), as a result, the heat flux is only 20 % higher than the reference. The flame temperature of Al/CuO composite with all carbon materials addition is roughly the same at ~2500 K, which is slightly lower compared to reference Al/CuO (2800 K) [38,39]. In short, among the three-carbon materials, only GO promotes the energy delivery rate of Al/CuO composite. We may conclude that the observed effect is more related to the reason is more related to the energetic property of GO rather than the aggregation state of Al NPs. To further observe the effect of GO addition on Al agglomeration, we take a closer look at the flame front.

3.4. *Effects of GO addition on the Al agglomeration*

The flame front and Al agglomerating process of reference Al/CuO composites, and Al/CuO with Al@GO or Al@rGO were observed by a microscopic imaging system with pyrometry. The typical snapshots and their corresponding temperature maps are shown in Fig. 7a-f (more details in the supporting videos). The Al/CuO composite without the addition of GO or rGO clearly generates much larger agglomerations compared to the GO or rGO containing cases. As we mentioned previously, GO or rGO, because of gas generation, can disperse the Al NPS and reduce the aggregations before combustion, thus decreasing the negative effects of sintering. The combustion products from both cases were collected and characterized by SEM/EDS. The combustion products are Al_xO_y with Cu caps, and are covered with much smaller Cu particles (from vapor condensation), as evident in the EDS results in Fig. S3. The size distributions of combustion products are also analyzed and shown in Fig. 7g-i. The average combustion product size of GO and rGO containing cases is 18 μm and 20 μm, respectively, which is approximately 2X smaller compared to the reference Al/CuO (34 μm). Smaller degree of agglomeration due to gas dispersal enables a higher degree of reaction, also making the flame front thinner with higher heat feedback to the unburnt materials from the flame front [11,31]. We also observed that the burning of GO is darker (Fig. 7b) compared to the burning of Al agglomerations (2600 K), indicating its lower flame temperature (< 2000 K). It is noted that the burning of GO containing composite is much brighter compared to rGO, confirming its superior energetic properties with more heat release, consistent with the evidence is shown in TG/DSC results in Fig. 3, making GO a favorable carbon additive that can be incorporated into Al/CuO composite at low mass fractions to boost the overall energy delivery rate.

The flame front and Al agglomerating process of Al/CuO composites with physically added GO or rGO were also observed by a microscopic imaging system with pyrometry, and the results are shown in Fig. S4. The combustion products are also collected and characterized by SEM/EDS (Fig. S5). The results show no apparent differences in the size

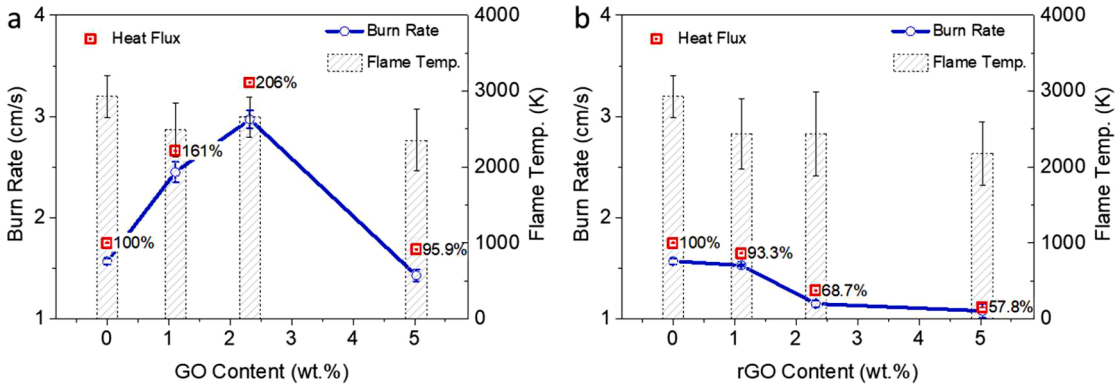

Fig. 5. Burn rate, flame temperature, and heat flux of Al/CuO composites with Al@GO (a) and Al@rGO (b) as functions of weight percentages of GO or rGO. With the addition of GO or rGO content, the Al/CuO content is decreasing from 90 wt % to 85 wt % while the polymer content is fixed at 10 wt %. The heat flux is normalized to Al/CuO with reference Al.

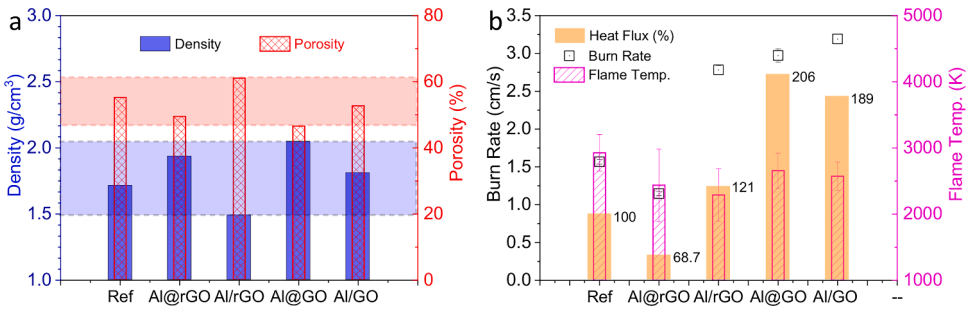

Fig. 6. Density/porosity (a) and burn rate, flame temperature, and heat flux of different Al/CuO composites with reference Al, Al@rGO, Al/rGO, Al@GO, and Al/GO. Note: Al@GO is a pre-assembled composite while Al/GO is a physical mixture of GO. The theoretical density of Al/CuO composite (with 10 wt % polymers) is estimated as 3.83 g/cm^3. The carbon materials content in all the composite sticks is fixed as 2.5 wt %. The heat flux is normalized to Al/CuO with reference Al.

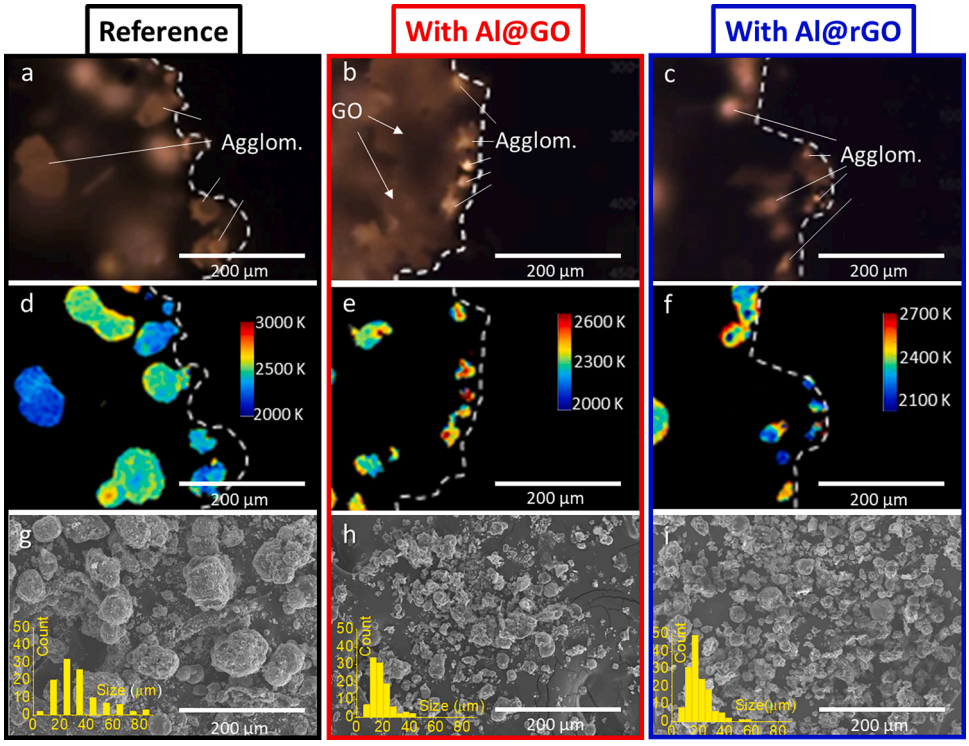

Fig. 7. Microscopic imaging snapshots (a, b, and c), their corresponding temperature maps (d, e, and f), SEM images of their post-combustion products (g, h, and i), and their size distributions (inserts in g, h, and i) of Al/CuO composites with reference Al (a, d, and g), and Al@GO (b, e, and h). GO or rGO content is 2.5 wt %. Note: "Agglom." stands for agglomerations.

distributions of the post-combustion products between pre-assembled Al@GO/CuO or Al@rGO/CuO composites, and the physically mixed Al/CuO/GO or Al/CuO/rGO composites, further confirming the pre-assembling between Al and GO is not essential in impacting combustion products, while physically added GO already can reduce the agglomeration of Al NPs and promote the reaction between Al and CuO.

4. Conclusions

In this study, we employed graphene-like carbon-based additives, i.e., GO and rGO, into free-standing Al/CuO composites. We found that GO is more efficient in promoting the flame propagation of Al/CuO composites. GO releases heat and gas upon disproportionation at low temperatures (~200 °C) that can increase the ignitibility of Al NPs and disperse Al NPs better. With just 2.5 wt % GO addition, the Al/CuO composite can have a 2x higher burn rate and energy delivery rate, whereas the addition of rGO will reduce its burn rate and energy delivery rate compared to the reference Al/CuO. Through a microscopic imaging system, we observed 2X smaller agglomerations formed from the GO and rGO containing cases compared to the reference Al/CuO, confirming both GO and rGO also can increase the dispersion and reduce the aggregations of Al NPs. Though both GO and rGO can reduce the agglomeration size of Al NPs, GO is more energetic with heat and gas release at low temperature, granting it the ability to increase the ignitability of Al NPs and promote the energy delivery of Al/CuO composite.

Author contributions

The manuscript was written through the contributions of all authors. All authors have approved the final version of the manuscript.

Supporting information

The following files are available free of charge.

XPS and Raman results of the GO and rGO. SEM and EDS images of the post-combustion products of the different Al/CuO composites with

reference Al, Al@GO, and Al@rGO. (PDF)

Declaration of Competing Interest

On behalf of all the authors, we declare no conflict of interest. This work is original and has not been considered for publication elsewhere.

Acknowledgment

We gratefully acknowledge support from ONR and AFOSR. We also thank the CFAMM at the University of California, Riverside, for their microscopy support.

Supplementary materials

Supplementary material associated with this article can be found, in the online version, at doi:10.1016/j.combustflame.2023.113095.

References

[1] E.L. Dreizin, Metal-based reactive nanomaterials, Prog. Energ. Combust. 35 (2009) 141–167.
[2] W. Wang, H. Li, M. Zhang, F. Zhao, S. Xu, C. Wang, Z. Qin, T. An, K. Xu, Effects of oxidizer and architecture on the thermochemical reactivity, laser ignition and combustion properties of nanothermite, Fuel 314 (2022), 123141.
[3] J. Xu, Y. Chen, W. Zhang, Z. Zheng, C. Yu, J. Wang, C. Song, J. Chen, X. Lei, K. Ma, Direct ink writing of nAl/pCuO/HPMC with outstanding combustion performance and ignition performance, Combust. Flame 236 (2022), 111747.
[4] M. Comet, C. Martin, F. Schnell, D. Spitzer, Nanothermite foams: from nanopowder to object, Chem. Eng. J. 316 (2017) 807–812.
[5] F. Sevely, X. Liu, T. Wu, F. Mesnilgrente, B. Franc, S. Assié-Souleille, X. Dollat, C. Rossi, Effect of process parameters on the properties of direct written gas-generating reactive layers, ACS Appl. Polym. Mater. 3 (2021) 3972–3980.
[6] K. Ryan Bratton, K.J. Hill, C. Woodruff, C. Cagle, M.L. Pantoya, J. Abraham, L. Wei, P. Dube, Tailoring impact debris dispersion using intact or fragmented thermite projectiles, J. Appl. Phys. 128 (2020), 155108.
[7] R.A. Yetter, G.A. Risha, S.F. Son, Metal particle combustion and nanotechnology, Proc. Combust. Inst. 32 (2009) 1819–1838.
[8] K. Shi, X. Guo, L. Chen, S. Huang, L. Zhao, J. Ji, X. Zhou, Alcohol-thermal synthesis of approximately core-shell structured Al@CuO nanothermite with improved heat-release and combustion characteristics, Combust. Flame 228 (2021) 331–339.
[9] W. He, J.Y. Lyu, D.Y. Tang, G.Q. He, P.J. Liu, Q.L. Yan, Control the combustion behavior of solid propellants by using core-shell Al-based composites, Combust. Flame 221 (2020) 441–452.
[10] Q. Luo, G. Liu, M. Zhu, X. Jiang, Constant volume combustion properties of Al/Fe2O3/RDX nanocomposite: the effects of its particle size and chemical constituents, Combust. Flame 238 (2022), 111938.
[11] H. Wang, D.J. Kline, P. Biswas, M.R. Zachariah, Connecting agglomeration and burn rate in a thermite reaction: role of oxidizer morphology, Combust. Flame 231 (2021), 111492.
[12] J.J. Granier, M.L. Pantoya, Laser ignition of nanocomposite thermites, Combust. Flame 138 (2004) 373–383.
[13] J. Hübner, M. Klaumünzer, M. Comet, C. Martin, L. Vidal, M. Schäfer, C. Kryschi, D. Spitzer, Insights into combustion mechanisms of variable aluminum-based iron oxide/-hydroxide nanothermites, Combust. Flame 184 (2017) 186–194.
[14] K.T. Sullivan, J.D. Kuntz, A.E. Gash, The role of fuel particle size on flame propagation velocity in thermites with a nanoscale oxidizer, Propellants Explos. Pyrotech. 39 (2014) 407–415.
[15] N. Zohari, M.H. Keshavarz, S.A. Seyedsadjadi, The advantages and shortcomings of using nano-sized energetic materials, Cent. Eur. J. Energ. Mat. 10 (2013) 135–147.
[16] K.T. Sullivan, N.W. Piekiel, C. Wu, S. Chowdhury, S.T. Kelly, T.C. Hufnagel, K. Fezzaa, M.R. Zachariah, Reactive sintering: an important component in the combustion of nanocomposite thermites, Combust. Flame 159 (2012) 2–15.
[17] P. Chakraborty, M.R. Zachariah, Do nanoenergetic particles remain nano-sized during combustion? Combust. Flame 161 (2014) 1408–1416.
[18] J. Jiang, P. Chen, J. Qiu, W. Sun, S.A. Chizhik, A.A. Makhaniok, G.B. Melnikova, T. A. Kuznetsova, Dynamic mechanical contact behaviors and sintering mechanism of Al nanoparticles subjected to high-speed impact, Mater. Chem. Phys. 273 (2021), 125111.
[19] G.C. Egan, T. LaGrange, M.R. Zachariah, Time-resolved nanosecond imaging of nanoscale condensed phase reaction, J. Phys. Chem. C 119 (2015) 2792–2797.
[20] H. Wang, D.J. Kline, M.R. Zachariah, In-operando high-speed microscopy and thermometry of reaction propagation and sintering in a nanocomposite, Nat. Commun. 10 (2019) 3032.
[21] Y. Jiang, A.R. Demko, J. Baek, X. Shi, L. Vallez, R. Ning, X. Zheng, Facilitating laser ignition and combustion of boron with a mixture of graphene oxide and graphite fluoride, Appl. Energy Combust. Sci. 1 (2020), 100013.
[22] J. Wang, W. Cao, R. Liu, R. Xu, X. Chen, Graphite fluoride as a new oxidizer to construct nano-Al based reactive material and its combustion performance, Combust. Flame 229 (2021), 111393.
[23] H.S. Kim, J.H. Kim, K.J. Kim, S.H. Kim, Tuning the ignition and combustion properties of nanoenergetic materials by incorporating with carbon black nanoparticles, Combust. Flame 194 (2018) 264–270.
[24] M.D. Garrison, S.G. Wallace, L.C. Baldwin, Z. Guo, L. Kuo, J.E. Estevez, A. L. Briseno, M.C. Hersam, A.J. Baca, Accelerated decomposition kinetics of ammonium perchlorate via conformal graphene coating, Chem. Mater. 33 (2021) 9608–9617.
[25] Y. Wang, F. Li, Y. Shen, C.A. Wang, Z. Zhang, J. Xu, Y. Ye, R. Shen, Fabrication of high electrostatic safety metastable Al/CuO nanocomposites doped with nitro-functionalized graphene with fast initiation ability and tunable reaction performance, Combust. Flame 233 (2021), 111580.
[26] X. Ma, S. Gu, Y. Li, J. Lu, G. Yang, K. Zhang, Additive-free energetic film based on graphene oxide and nanoscale energetic coordination polymer for transient microchip, Adv. Funct. Mater. 31 (2021), 2103199.
[27] J. Shen, Z. Qiao, J. Wang, G. Yang, J. Chen, Z. Li, X. Liao, H. Wang, M.R. Zachariah, Reaction mechanism of Al-CuO nanothermites with addition of multilayer graphene, Thermochim. Acta 666 (2018) 60–65.
[28] Z. Yi, Y. Cao, J. Yuan, C. Mary, Z. Wan, Y. Li, C. Zhu, L. Zhang, S. Zhu, Functionalized carbon fibers assembly with Al/Bi2O3: a new strategy for high-reliability ignition, Chem. Eng. J. 389 (2020), 124254.
[29] Y. Jiang, S. Deng, S. Hong, S. Tiwari, H. Chen, K.I. Nomura, R.K. Kalia, A. Nakano, P. Vashishta, M.R. Zachariah, X. Zheng, Synergistically chemical and thermal coupling between graphene oxide and graphene fluoride for enhancing aluminum, Combust. ACS Appl. Mater. Inter. 12 (2020) 7451–7458.
[30] Y. Jiang, S. Deng, S. Hong, J. Zhao, S. Huang, C.C. Wu, J.L. Gottfried, K.I. Nomura, Y. Li, S. Tiwari, R.K. Kalia, Energetic performance of optically activated aluminum/graphene oxide composites, ACS Nano 12 (2018) 11366–11375.
[31] H. Wang, D.J. Kline, M.C. Rehwoldt, M.R. Zachariah, Carbon fibers enhance the propagation of high loading nanothermites: *in situ* observation of microscopic combustion, ACS Appl. Mater. Inter. 13 (2021) 30504–30511.
[32] L. Zhou, N. Piekiel, S. Chowdhury, M.R. Zachariah, Time-resolved mass spectrometry of the exothermic reaction between nanoaluminum and metal oxides: the role of oxygen release, J. Phys. Chem. C 114 (2010) 14269–14275.
[33] G. Jian, N.W. Piekiel, M.R. Zachariah, Time-resolved mass spectrometry of Nano-Al and Nano-Al/CuO thermite under rapid heating: a mechanistic study, J. Phys. Chem. C 116 (2012) 26881–26887.
[34] R.J. Jacob, D.J. Kline, M.R. Zachariah, High speed 2-dimensional temperature measurements of nanothermite composites: probing thermal vs. Gas generation effects, J. Appl. Phys. 123 (2018), 115902.
[35] D.J. Kline, Z. Alibay, M.C. Rehwoldt, A. Idrogo-Lam, S.G. Hamilton, P. Biswas, F. Xu, M.R. Zachariah, Experimental observation of the heat transfer mechanisms that drive propagation in additively manufactured energetic materials, Combust. Flame 215 (2020) 417–424.
[36] D. Krishnan, F. Kim, J. Luo, R. Cruz-Silva, L.J. Cote, H.D. Jang, J. Huang, Energetic graphene oxide: challenges and opportunities, Nano Today 7 (2012) 137–152.
[37] H. Wang, J. Shen, D.J. Kline, N. Eckman, N.R. Agrawal, T. Wu, P. Wang, M. R. Zachariah, Direct writing of a 90 wt % particle loading nanothermite, Adv. Mater. 31 (2019), 1806575.
[38] D.S. Sundaram, V. Yang, V.E. Zarko, Combustion of nano aluminum particles (Review), Combust. Explos. Shock Waves 51 (2015) 173–196.
[39] J.M. Epps, J.P. Hickey, J.Z. Wen, Modelling reaction propagation for Al/CuO nanothermite pellet combustion, Combust. Flame 229 (2021), 111374.